



# High Temperature Oxidation of Additively Manufactured Structural Alloys

Daniel Monceau, Michel Vilasi

## ► To cite this version:

Daniel Monceau, Michel Vilasi. High Temperature Oxidation of Additively Manufactured Structural Alloys. JOM Journal of the Minerals, Metals and Materials Society, 2022, 74 (4), pp.1659-1667. 10.1007/s11837-022-05198-z . hal-03658142

**HAL Id: hal-03658142**

**<https://hal.science/hal-03658142>**

Submitted on 3 May 2022

**HAL** is a multi-disciplinary open access archive for the deposit and dissemination of scientific research documents, whether they are published or not. The documents may come from teaching and research institutions in France or abroad, or from public or private research centers.

L'archive ouverte pluridisciplinaire **HAL**, est destinée au dépôt et à la diffusion de documents scientifiques de niveau recherche, publiés ou non, émanant des établissements d'enseignement et de recherche français ou étrangers, des laboratoires publics ou privés.




## Open Archive Toulouse Archive Ouverte (OATAO)

OATAO is an open access repository that collects the work of Toulouse researchers and makes it freely available over the web where possible

This is an author's version published in: <http://oatao.univ-toulouse.fr/28993>

**Official URL:** <https://doi.org/10.1007/s11837-022-05198-z>

### **To cite this version:**

Monceau, Daniel  and Vilasi, Michel *High Temperature Oxidation of Additively Manufactured Structural Alloys*. (2022) JOM Journal of the Minerals, Metals and Materials Society, 74 (4). 1659-1667. ISSN 1047-4838

Any correspondence concerning this service should be sent  
to the repository administrator: [tech-oatao@listes-diff.inp-toulouse.fr](mailto:tech-oatao@listes-diff.inp-toulouse.fr)

# High Temperature Oxidation of Additively Manufactured Structural Alloys

DANIEL MONCEAU <sup>1,3</sup> and MICHEL VILASI<sup>2</sup>

1. CIRIMAT, CNRS, ENSIACET INPT, 4, allée Emile Monso, BP 44362, 31030 Toulouse Cedex4, France. 2. Université de Lorraine, CNRS, IJL, 54000 Nancy, France. 3. e mail: daniel.monceau@toulouse.inp.fr

Metal alloys produced by additive manufacturing have specific microstructures and compositions. Their microstructure is generally out of equilibrium, textured, and inhomogeneities can be observed. They can have pores and nano-inclusions. The contents of volatile elements may deviate from the nominal composition. These alloys often experience significant internal stresses and present fairly rough surfaces depending on the process used. HIPping these alloys modifies their microstructure and defects. This literature review shows that open porosity can lead to much higher oxidation kinetics than dense materials, with very deep internal oxide penetrations. Nevertheless, when fabricated with optimized parameters, LBM- or EBM-alloys, such as TA6V, 718, or 316L, can behave as well as, or even better than, wrought alloys. The roughness of the surface is not necessarily problematic, but it can lead to local breakaway phenomena and premature spalling on some alloys. It has been verified that the nature of the grain boundaries strongly affects the intergranular oxidation. The effect of chemical segregations on the protective nature of the outer oxide layer has also been reported. Today, too few studies have been devoted to the effect of raw and pre-oxidized surface states after HIP on cyclic oxidation and on hot corrosion of these alloys.

## INTRODUCTION

The alloys produced by additive manufacturing (AM)<sup>1,2</sup> may have been designed for specific processes, but in general, they use standard chemical compositions of alloys already used in industry, and produced by casting or forging. However, these alloys have special characteristics that can affect their resistance to oxidation at high temperatures. Therefore, most of the work published to date reports standard characterizations of resistance to oxidation at high temperature, intended to demonstrate that the material does not have strongly degraded properties compared to those produced by conventional processes. Most of these studies deal with alloys fabricated by laser beam melting (LBM) and electron beam melting (EBM) of powder bed processes. In this article, we present the chemical

and microstructural characteristics of alloys resulting from additive manufacturing that we believe to be important in relation to resistance to oxidation. We then review the experimental results which do or do not demonstrate an influence of these characteristics. We also highlight topics that are not yet well documented.

## SPECIAL CHARACTERISTICS OF AM ALLOYS THAT CAN INFLUENCE OXIDATION AT HIGH TEMPERATURE

The particular characteristics of metal alloy parts resulting from additive manufacturing relate to the chemical composition and its homogeneity, the microstructure, the surface condition and the surface particular morphology, the complex geometry of the parts, and, in particular, the possible thinness of their walls, the residual stresses, and finally certain characteristic defects.<sup>1,2</sup> Figure 1 illustrates some characteristics of AM alloys with their

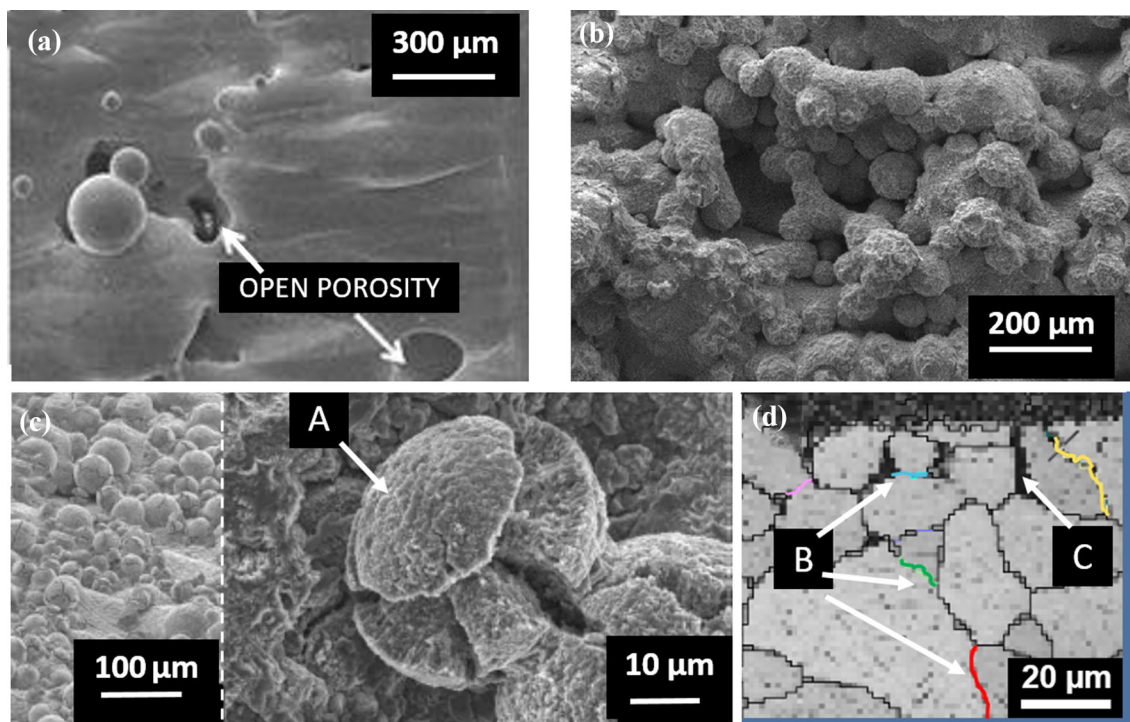


Fig. 1. Effect of the microstructural characteristics of materials from AM on their oxidation behavior: (a) open porosity, 718 LBM<sup>3</sup> (SEM-SE), (b) roughness, 718 EBM (SEM-SE),<sup>4</sup> (c) unmelted powder particles fully oxidized (A), TA6V EBM (SEM-SE),<sup>5</sup> (d) special grain boundaries (B in blue, green, red, yellow) without any intergranular oxidation (C in black) (electron backscatter diffraction).<sup>6</sup>

consequences on high-temperature oxidation. Nominal compositions of all the alloys cited in this paper are given in Table I.

### EFFECT OF CHEMICAL COMPOSITION

The various atomization processes (by gas jet, water jet, etc.) can lead to significantly different compositions from the alloy powder intended for additive manufacturing. If the contents of the major elements comply with the desired characteristic values, those of the minor elements may, on the other hand, diverge depending on the process for making the powder. This is, for example, the case with manganese, the content of which varied from 0.1 wt.% to 0.5 wt.% within two types of powder used by Tobar et al.<sup>7</sup> to produce 316L steels by laser fusion (Table I). In addition, the chemical composition of LBM or EBM alloys may differ slightly from the composition of the precursor powder. Some elements, which can volatilize, are important for oxidation and corrosion. Note in particular the case of aluminum, which allows the formation of a protective oxide layer of alumina, provided it is in sufficient concentration in the alloy. Juechter et al. studied the compositional variations during EBM of a TA6V titanium alloy, and showed loss of Al during processing.<sup>8</sup> Finally, during manufacturing, it is difficult to guarantee that the gas of the chamber is completely inert.

Additive manufacturing processes use a flow of Ar (or even N<sub>2</sub>) directed to the melting zone, or are carried out under secondary vacuum. Nevertheless, gases such as O<sub>2</sub>, H<sub>2</sub>, H<sub>2</sub>O, N<sub>2</sub>, CO, and CO<sub>2</sub> can cause contamination of the material and powder particles which will be recycled.<sup>9</sup> These gases are impurities in the shielding gases used, but they can also desorb from the metal during its melting. Given the nature of the gases and the vacuum levels used, one can expect partial oxygen pressures of 10<sup>-5</sup> atm to 10<sup>-8</sup> atm, which are sufficient to oxidize most metals and, in particular, Al, Ti, Zr, Si, and Cr; however, the oxidation times are short. Yu et al.<sup>10</sup> demonstrated that fine particles of Al<sub>2</sub>O<sub>3</sub> may have formed during the fabrication of alloy 718 by the EBM and LBM processes. These particles have been identified as being sites for the nucleation of Ti-Nb carbides.

Titanium alloys can be expected to be sensitive to the printing atmosphere, due to the reactivity of titanium with oxygen, nitrogen, and carbon. This has been shown for the TA6V alloy produced by the EBM process. An increase of 0.11 wt.% oxygen was measured on TA6V powder recycled 21 times.<sup>11</sup> This is important for titanium alloys, whose microstructure and mechanical properties are strongly affected by a few hundred ppm of oxygen.<sup>12</sup> The recycled powder particles accumulate pollution by oxidation cycle after cycle. The recyclability of powders has been the subject of numerous studies, for example,

**Table I. Nominal composition of alloys referenced in this paper (wt.%)**

Alloy	Fe	Ni	Ti	Cr	Al	Nb	Mo	W	Mn	Co	Cu	Si	C	S	P	B
718	11.1-24.6	50.0-55.0	0.65-1.15	17.0-21.0	0.20-0.8	4.75-5.50	2.80-3.30		0.35 *	1.0 *	0.30 *	0.35 *	0.08 *	0.015 *	0.015 *	0.006 *
625	5.0 *	58.0 **		20.0-23.0	0.40 *		8.0-10.0		0.50 *	1.0 *		0.50 *	0.10 *	0.015 *	0.015 *	
HX	18.5	47.3 **		22			9	0.6	0.5	1.5		0.5	0.1			
316 L	63.4-70.445	10.5-13.0		16.5-18			2.0-2.5		2 *	0.1 *		1 *	0.02	0.015 *	0.045 *	
Alloy	Fe	Ni	Ti	Al	Mg	V	Mn	Cu	Si	Sc	Zr	Zn	C	O		
TA6V ELI	0.3 *		88.8-91	5.50-6.50		3.50-4.50							0.08 *	0.13 *		
Scalm-alloy	0.4 *	0.15 *		91.6-94.9	4.0-4.9	0.05 *	0.3-0.8	0.1 *	0.4 *	0.6-0.8	0.2-0.5	0.25 *		0.05 *		
															*Max, **Min	

\*Max, \*\*Min

for titanium alloy TA6V and superalloy 718.<sup>11,13-15</sup> The results show overall that it is possible to maintain a very low pollution with the LBM and EBM processes for these two alloys, even after dozens of cycles.

Impurities are very important for certain properties of alloys. In the field of high-temperature oxidation, with conventionally processed materials, it is well known that the sulfur content, at the ppm or even at the sub-ppm level, affects the adhesion of alumina to Ni-based superalloys (e.g.,<sup>16</sup>) As a consequence, the kinetics of cyclic oxidation increases with the level of S (in terms of metal consumption). Carbon can also play a role.<sup>17</sup> The reactive elements (Hf, Y, Zr, Ce, and La) interact with these species,<sup>18</sup> and then also affect the oxidation behavior in thermal cycling. It has also been shown that phosphorus can affect intergranular oxidation in alloy 718.<sup>19</sup>

In 2014, Unocic et al.<sup>20</sup> published a first study on the cyclic oxidation characterization of AM-alloy 718. Following these pioneering works carried out at ORNL, Romedenne et al.<sup>21</sup> studied the cyclic oxidation in air at 950°C of the Hastelloy X alloy, produced by LBM and EBM, by comparing their behavior with that of the wrought alloy. They found that the oxide scale of the Hastelloy X alloy produced by EBM and LBM spalled faster than the wrought alloy. This result was attributed to the formation of a thin layer of SiO<sub>2</sub> at the metal/Cr<sub>2</sub>O<sub>3</sub> interface.

In 2021, Sanviemvongsak<sup>22</sup> showed that the LBM 718 alloy exhibited a highly degraded cyclic oxidation resistance compared to the EBM 718 and the wrought 718 alloys, while these alloys exhibit similar isothermal oxidation behaviors. No explanation could be found in the microstructural differences of the three alloys. It was instead proposed that the level of free sulfur (S dissolved in the gamma phase) was the explanation, and it was shown by a thermodynamic calculation that the small concentration of Mn could explain the fact that the alloy LBM had a higher level of free S (Fig. 2). These examples show that, first, cyclic oxidation experiments are required in addition to isothermal experiments, and, second, the level of impurities should be controlled at the level of 0.1–100 ppm, depending on the elements. This includes the level of S and C in Ni-base superalloys and steels, and also of reactive elements known to trap S and C, and of some elements with the same properties, such as Mn. This includes also Al, Ti, and Si elements in Ni- or Fe-based chromia formers because they can form internal and intergranular oxides (Fig. 3).<sup>23</sup>

## EFFECT OF MICROSTRUCTURE AND CHEMICAL HOMOGENEITY

Even when their level of porosity is very low, alloys from additive manufacturing can have specific microstructures that can affect high-temperature

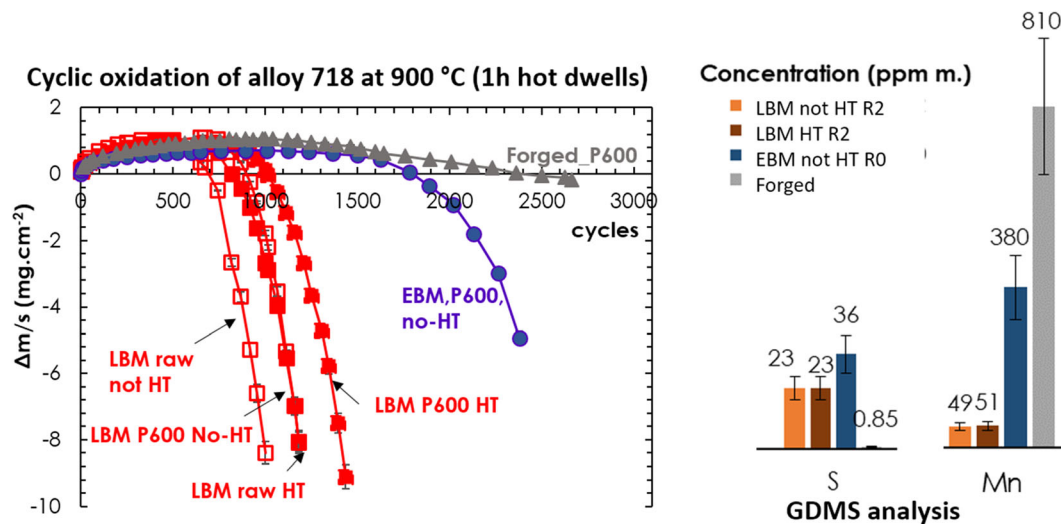


Fig. 2. Effect of alloy 718 impurities on cyclic oxidation kinetics. The worst behavior is obtained for the LBM-718 alloy which may not have enough Mn to compensate for its S level. The best behavior is obtained for the forged alloy 718 which has a low S concentration and a lot of Mn (see text).<sup>22</sup> HT heat-treated, P600 ground to P600 paper finish, raw not ground.

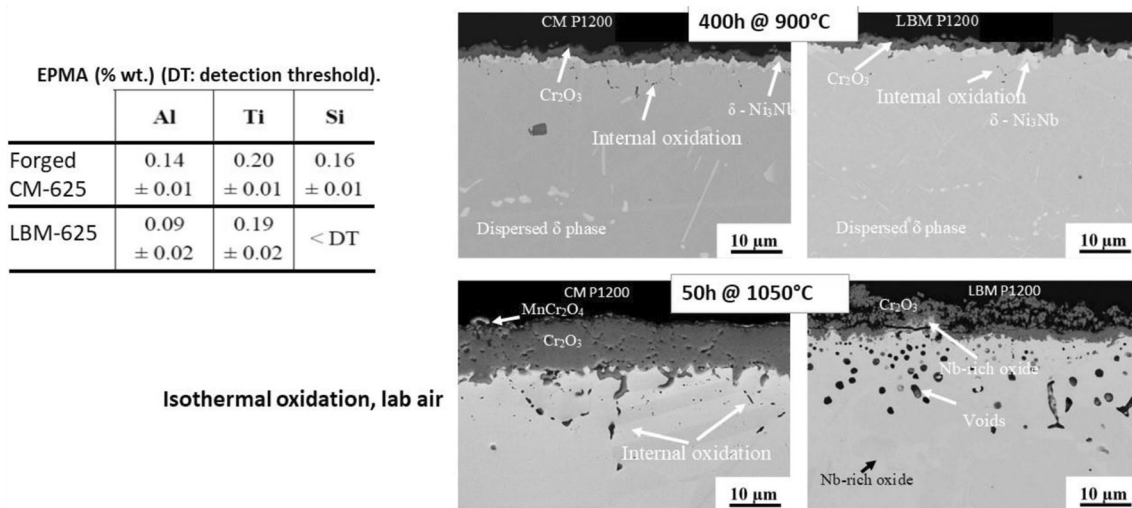


Fig. 3. Effect of powder composition and AM processing on the composition on internal and intergranular oxidation of alloy 625 (after).<sup>23</sup> Less Al in LBM-625 than in wrought 625 leads to less internal and intergranular oxidation at 900°C and 1050°C.

oxidation. Non-equilibrium microstructures can be generated: for example,  $\alpha'$  martensite in Ti alloys, or the absence of hardening precipitates in Ni-based alloys, or chemical segregations, for example, Nb, Ti, and Mo in interdendritic zones of alloy 718, which can cause precipitation of Laves phases.<sup>24,25</sup> Morphological anisotropies and crystallographic texturing are also often observed. Parts can be used as raw materials, as processed or annealed, or exposed to high isostatic pressing (HIP). HIP can erase all or part of these microstructural peculiarities.

These differences in microstructures can influence the homogeneity of the outer oxide layer, intergranular oxidation, or even the diffusion of oxygen into the metal matrix in the case of titanium

alloys.<sup>26</sup> For example, it has been shown for standard manufacturing processes that the texturing of alloys influences the number of special grain boundaries, and that these are much more resistant to intergranular oxidation.<sup>27,28</sup> In particular,  $\Sigma 3$  grain boundaries have better resistance to intergranular oxidation. Sanviemvongsak et al.<sup>4</sup> studied the link between the nature of grain boundaries resulting from additive manufacturing and the kinetics of intergranular oxidation. Samples of alloy 718 from LBM- or EBM-optimized fabrication showed external oxidation kinetics and mass gains similar to wrought samples. On the other hand, intergranular oxidation differences were noted. More recently, it was shown by electron backscatter diffraction analyzes on samples oxidized over long periods of time

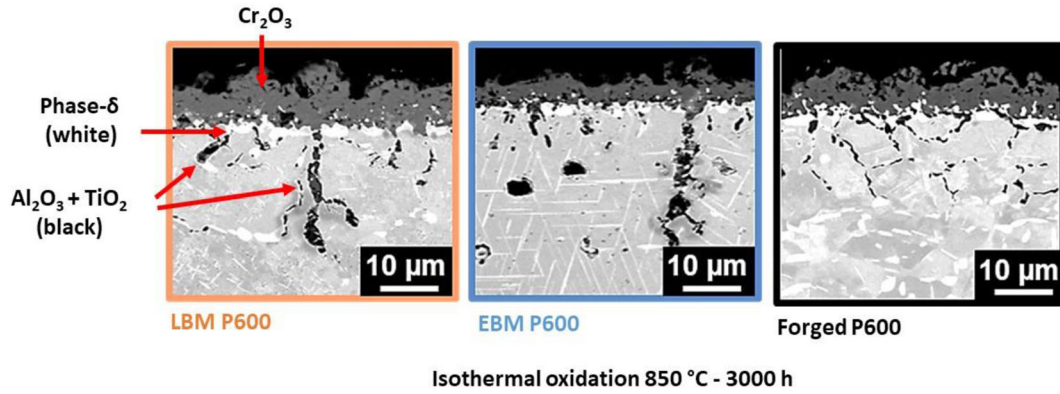


Fig. 4. Intergranular oxidation of alloy 718. Statistical evaluations showed that AM alloys present thicker intergranular oxidation, the same average depth of intergranular oxidation than forged alloy, but with deeper occurrences.<sup>6</sup>

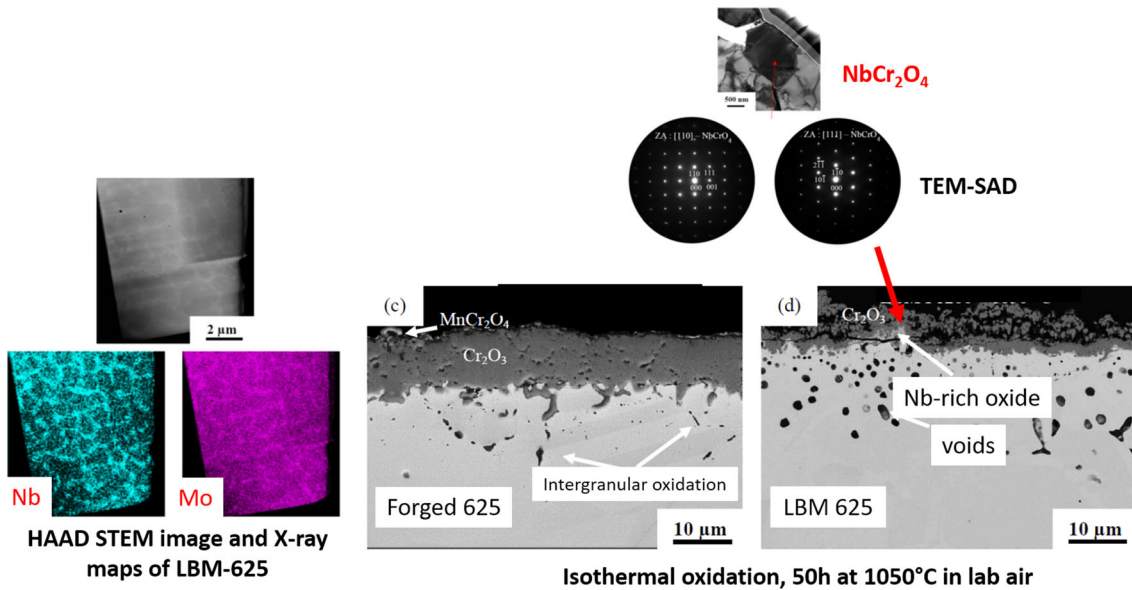


Fig. 5. Effect of chemical segregation during AM processing (Nb and Mo) on the oxidation of alloy 625. Nb and Mo segregation leads to local formation of Nb-oxide and volatile Mo-oxides leaving voids in the substrate and decreasing the protectiveness of chromia scale (after<sup>23</sup>).

at 850°C, that these differences were in part due to different special grain boundary densities in these different samples (Fig. 4).<sup>6</sup>

Ramenatte et al.<sup>23</sup> compared the air oxidation of alloy 625 produced by LBM or casting and rolling. The LBM alloy exhibits a cellular microstructure with significant segregations of Nb and Mo. At 900°C, this does not impact the resistance to oxidation, but at 1050°C, a marked deterioration in the oxidation behavior of the LBM alloy is observed, with the formation of numerous pores under the oxide layer and a significant amount of  $\text{Nb}_{1.5}\text{Cr}_{0.5}\text{O}_4$  rutile in the internal part of the oxide layer (Fig. 5). Juillet et al.<sup>29</sup> had previously found an opposite effect when comparing cast and LBM alloys. The higher  $\delta\text{-Ni}_3\text{Nb}$  phase level in the cast alloy resulted in the presence of more  $\text{Nb}_2\text{O}_5$  in the oxide layer which was then less protective. Siri

et al.<sup>30</sup> have compared the isothermal oxidation behavior of 316L steel made by LBM to the isothermal oxidation behavior of a wrought alloy. They found slower oxidation kinetics for the LBM alloy between 700°C and 1000°C, and attributed this improvement to an enhanced diffusion of Cr to the surface.

Regarding the TA6V alloy, the microstructure is closely dependent on the AM technique used, as illustrated in Fig. 2, showing the microstructures of two materials studied by Casadebaigt et al.,<sup>5,26</sup> produced, respectively, by EBM and LBM. The main problem with titanium alloys is their embrittlement due to oxygen dissolution at high temperature.<sup>12</sup> The temperature of use of TA6V (<500°C) is low compared to its melting temperature, so we can therefore expect a significant contribution of short-circuit diffusion at internal interfaces on the

diffusion of oxygen in the metal matrix. Despite this, Casadebaigt et al.<sup>26</sup> showed that the fineness of the microstructure did not influence the kinetics of oxygen penetration. This was shown by comparing the behavior of TA6V produced by conventional methods, by LBM and EBM, with thin microstructures and after HIP with a much coarser microstructure.

### EFFECT OF PROCESSING DEFECTS AND HIP

The manufacture of an alloy with non-optimized parameters can lead to the presence of defects which can greatly influence the oxidation kinetics. Jia et al.<sup>3</sup> studied the high-temperature oxidation of samples of the LBM-718 alloy with high energy densities, which led to the presence of open porosity in the samples and to mass gains very important during high-temperature oxidation. Sanviemvongsak et al.<sup>4</sup> also studied the oxidation of alloy 718 manufactured by LBM and EBM, but with optimized parameters, and few defects were observed. They showed that the LBM, EBM, and forged alloys then had very similar oxidation kinetics when the surface conditions were equivalent (P600 polishing). For a material with pores, a HIP treatment can lead to an improvement in the resistance to oxidation at high temperature by densifying the material, but the HIP can also lead to microstructural changes, such as precipitation at the grain boundaries which can affect intergranular oxidation, as has been shown on alloy 718 fabricated by LBM.<sup>31</sup>

### EFFECT OF SURFACE ROUGHNESS

The powder particles used for additive manufacturing have diameters generally between 15  $\mu\text{m}$  and 120  $\mu\text{m}$ , with a typical particle size of a TA6V powder for the EBM process being  $70 \mu\text{m} \pm -25/+50 \mu\text{m}$  and a typical particle size of a Ni-base alloy powder for the LBM process being  $30 \mu\text{m} \pm 20 \mu\text{m}$ .<sup>32</sup> This leads to surface roughness which can be high ( $R_a$  of several tens of micrometers). There are “staircase” effects due to the fabrication by layer, with an effect of the fabrication angle. Sometimes, the presence of unmelted powder particles sintered on the surface (“satellites”), or metal droplets of very variable sizes, ejected from the molten bath to a previously molten and solidified layer of metal (“spatters”), are observed. It has been shown that, for alloy 718, roughness of EBM samples could lead to reactive surface areas 2–4 times higher than a flat surface.<sup>4</sup> When measuring the reactive surface area, one must be careful of hidden surfaces if a 3D-image analysis is used.<sup>5,33</sup> When the oxidation or corrosion kinetics are studied, it is therefore necessary to be particularly attentive to this parameter in order not to reach erroneous conclusions. For

example, in,<sup>4</sup> as processed additive manufacturing alloys exhibit higher oxidation kinetics than alloys forged or polished in terms of mass gains. However, this is only due to their higher reactive surface area. If the oxidation kinetics are characterized by the thickness of the oxide layer formed, or the thickness of the metal consumed, and this is what ultimately matters, there is no longer any difference between the 718 alloys forged, LBM or EBM, under isothermal oxidation conditions. These authors even noted that the EBM alloy exhibited slightly better behavior than forged, from measurements on polished samples. Ramenatte et al.<sup>23</sup> confirmed these results on alloy 625.

Casadebaigt et al.<sup>5</sup> studied the effect of surface roughness on a TA6V alloy obtained from LBM, EBM, or rolled. However, they also showed a specific behavior for this titanium alloy. Indeed, on a raw surface after additive manufacturing, the partially melted powder particles attached to the surface oxidize catastrophically. After an incubation time, the anionic growth of the rutile  $\text{TiO}_2$  layer and the strong increase in volume induced by the oxidation of titanium generated very high mechanical stresses in the powder particles, which caused their cracking and the acceleration of their oxidation. In this study, it was shown that the very rapid oxidation of the powder particles contributed about half of the mass gains recorded (Fig. 6).

The catastrophic oxidation of the Ti powder at the surface of AM part is a phenomenon which does not affect the health of the material. However, sometimes, the surface geometry can affect the nature, the kinetics, and the growth constraints of the layer and its adherence. In an atmosphere of catastrophic powdery carburization, called metal dusting, Vernouillet et al.<sup>34</sup> showed that the samples of alloy 625 LBM and LBM + HIP with rough surfaces, suffered greater mass losses than polished samples. In addition, the raw HIP samples showed large variations in behavior. Indeed, the significant roughness due to additive manufacturing, and the high grain sizes due to HIP, can cause greater localized depletion of Cr and thus lead to the formation of a spinel on the surface, which catalyzes the decomposition of CO and is less protective with respect to oxidation and carburization (Fig. 4). The spinel formation in convex surface areas has also been observed after 500 h of oxidation at 800°C of EBM-Hastelloy X.<sup>33</sup>

The roughness also affects the state of stress in the oxide layer and can lead to premature spalling of the oxide layers.<sup>35</sup> During their study on the cyclic oxidation kinetics of alloy 718, Sanviemvongsak et al.<sup>22</sup> observed that grinding with P600 paper of the surface of the LBM alloy delayed the catastrophic spallation of oxides during thermal cycles of 1 h at 900°C, but did not prevent it.

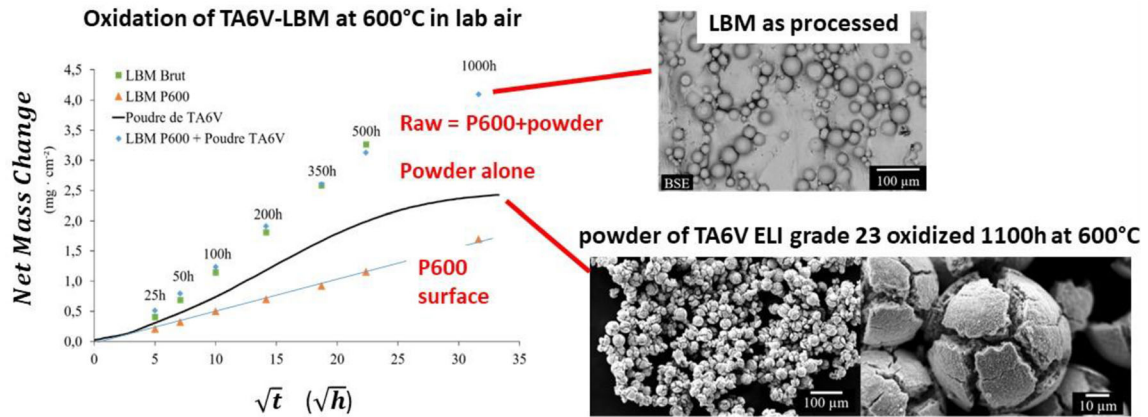


Fig. 6. Effect of TA6V powder oxidation at the surface of LBM-TA6V. Catastrophic oxidation of titanium powder leads to an initial large increase of mass gain. (after<sup>5</sup>).

## EFFECT OF RESIDUAL STRESSES

Due to the large temperature gradients during additive manufacturing, parts are subjected to high levels of residual elastic stresses. These can influence the reactivity of surfaces, and the diffusion to the core of the material. In particular, internal and intergranular oxidation, which itself generates significant strain due to the large increase in volume associated with oxidation, may depend on the initial presence of stresses from the manufacturing process. This has been shown by Bertali et al.<sup>36</sup> for a conventional 600 alloy tested at 480°C under an H<sub>2</sub> + H<sub>2</sub>O mixture, but this does not seem to have been reported to date for additive manufacturing materials.

## EFFECT OF COMPLEX GEOMETRIES AND THIN WALLS

One of the major interests of additive manufacturing is the possibility of manufacturing parts of complex geometry, with hidden surfaces inaccessible to machining. These complex geometries can have thin elements and thin walls, which can have several consequences on their chemical reactivity and mechanical behavior. First, hidden surfaces cannot receive all types of surface treatments. For example, grit blasting, shot blasting, and coating application can be difficult or impossible inside parts. This of course has an effect on the reactivity of the internal surfaces. Then, the morphology and the surface defects depend on their angle with respect to the direction of construction of the part. This influences the oxidation. For example, Li et al.<sup>28</sup> seem to show during preliminary results on an alloy 718 produced by EBM, that the fabrication angle affects the orientation of the grains and the density of grain boundaries, which would have a slight repercussion on the resistance to oxidation at high temperature. Finally, the fineness of some AM structures can make them susceptible to premature

exhaustion of alloying elements that protect against oxidation or corrosion at high temperature. In isothermal oxidation, if a protective layer of Al<sub>2</sub>O<sub>3</sub> or Cr<sub>2</sub>O<sub>3</sub> forms on a surface, this creates a Cr or Al depletion under the oxide layer. If the wall of the part is thin and at high temperature, the depletion profiles meet from the two surfaces of the wall, the core concentration decreases, and consequently that under the oxide layer also decreases. This can cause a “breakaway” phenomenon, that is, the formation of a less protective oxide layer formed from the other elements of the alloy, and faster growing by several orders of magnitude.<sup>37,38</sup> In the case of a titanium alloy, another thin wall effect exists, as oxygen diffuses in large quantities into the metal under the oxide layer and weakens it.<sup>12</sup> This effect is, of course, more dangerous on a thin wall.<sup>39</sup>

## EFFECT OF PREOXIDATION DURING HIGH ISOSTATIC PRESSURE TREATMENT (HIP)

The purpose of the HIP treatment carried out at high temperature and high hydrostatic pressure is to close the pores and defects formed during additive manufacturing. This heat treatment will also reduce or eliminate the internal stresses<sup>31</sup> and modify the microstructure (nature of the phases and grain size). It is carried out at a high temperature and under a very high pressure, typically 1000 bars. If the gas used is nitrogen or argon, these contain impurities of O<sub>2</sub> and H<sub>2</sub>O, which, due to the high pressure, can lead to significant surface oxidation. Nitrogen can also cause internal nitridation. Since the HIP treatment is carried out in a closed chamber, which may contain metal walls, graphite tools, and ceramic insulators, the reactivity of the metal alloys will also depend on the furnace used and on the total surface area of the samples treated at the same time in the chamber. No systematic study on this subject is available in the literature to our knowledge.

## ALLOYS DEVELOPED SPECIFICALLY FOR AM

New alloys with improved mechanical and chemical properties have been designed by exploiting the specificities of AM powder bed fusion processes to develop novel microstructures. This is, for example, the high mechanical performance Scalmetal<sup>®</sup> aluminum alloy, which has been patented by Airbus-APWorks GmbH, and which has been the subject of a comprehensive metallurgical study by Spierings et al.<sup>40</sup> Another example is given by Hong et al.<sup>41</sup> who reported a comparative study of the high-temperature oxidation of alloy 625 and of a 625/TiC composite, both developed by LMD. These authors report a surprising beneficial effect of the presence of TiC, but the oxidation kinetics are not compared to a forged 625 alloy, and the oxide layers are not observed in section to verify their thicknesses. These preliminary works need more extensive studies on reactivity.

## SUMMARY OF AM ALLOY PERFORMANCE AND CONCLUSIONS

1. Porosity and defects resulting from a lack of powder fusion, and also from gas trapping, lead to significant degradation of oxidation behavior<sup>3</sup> if these defects are connected to the external surface. High-temperature oxidation reveals the open porosity. The oxidation kinetics increase, and also the consumption of protective alloying elements. This can lead to a premature breakaway phenomenon. In addition, the oxidation of cracks with the very significant increase in volume when the metal is transformed into oxide are sites of stress concentration and can lead to rupture.
2. The surface roughness, generally linked to the particle size distribution of the powders, increases the area of the reactive surface and therefore the quantity of oxide formed for fairly short times. The reactive surface area was observed to be multiplied by 4 for EBM-718 in comparison to a flat surface.<sup>4</sup> This increase in reactivity is transient and not necessarily detrimental to the part in terms of affected thickness, as has been seen in high-temperature oxidation of alloy 718,<sup>4</sup> but may lead to local breakaway, as observed on alloy 625<sup>23,34</sup> or Hastelloy X.<sup>33</sup>
3. The complexity of microstructures is inherent to the rate of the melting and cooling processes, which is conducive to elemental segregation. During high-temperature oxidation, these segregations could lead to the formation of non-protective oxides,<sup>23</sup> but there is a lack of experimental data on this point.
4. The nature of grain boundaries may be different from those observed in materials from conventional elaboration processes, due to increased

segregation, pore closures during HIP, texturing, and internal stresses, and this may affect high-temperature intergranular oxidation kinetics.<sup>6</sup>

5. The resistance to cyclic oxidation and hot corrosion has been scarcely reported in the literature.<sup>20–22</sup> On this subject, special attention must be paid to impurities and minor elements that can affect the adhesion of the oxide layers (S, C, reactive elements, sulfide-forming elements). The geometry of the surfaces may also greatly affect the stress state during thermal cycling. Furthermore, surface roughness could affect hot corrosion with melted salts. Here again, experimental data are missing.

To improve the performance of AM parts, it is first mandatory to produce materials without open porosity. Roughness is not necessarily a problem, but it must be evaluated with long-term oxidation tests until the appearance of the “breakaway” phenomenon, and under thermal cycling conditions to increase the level of stress in the oxide scale. Then, it is possible to consider heat treatments intended to reduce the residual stresses. HIP treatment helps to homogenize the chemical composition and at the same time reduces manufacturing defects. Chemical or electrochemical surface treatments can also be considered to reduce surface roughness when necessary, with the difficulty of accessing hidden surfaces.

## ACKNOWLEDGEMENTS

Tom Sanviemvongsak, Nicolas Ramenatte, Anabelle Vernouillet, Antoine Casadebaigt, Aurélie Vande Put, Stéphane Mathieu, Jonathan Hugues, Eric Andrieu, Sébastien Doublet are thanked for fruitful discussions.

## CONFLICT OF INTEREST

On behalf of all authors, the corresponding author states that there is no conflict of interest.

## REFERENCES

1. S. Gorsse, C. Hutchinson, M. Gouné, and R. Banerjee, *Sci. Technol. Adv. Mater.* 18(1), 584 <https://doi.org/10.1080/14686996.2017.1361305> (2017).
2. Y. Kok, X.P. Tan, P. Wang, M.L.S. Nai, N.H. Loh, E. Liu, and S.B. Tor, *Mater. Des.* 139, 565 <https://doi.org/10.1016/j.matdes.2017.11.021> (2018).
3. Q. Jia, and D. Gu, *J. Alloy. Compd.* 585, 713 (2014).
4. T. Sanviemvongsak, D. Monceau, and B. Macquaire, *Corros. Sci.* 141, 127 <https://doi.org/10.1016/j.corsci.2018.07.005> (2018).
5. A. Casadebaigt, J. Hugues, and D. Monceau, *Oxid. Met.* 90(5), 633 <https://doi.org/10.1007/s11085-018-9859-0> (2018).
6. T. Sanviemvongsak, D. Monceau, C. Desgranges, and B. Macquaire, *Corros. Sci.* 170, 108684 <https://doi.org/10.1016/j.corsci.2020.108684> (2020).
7. M.J. Tobar, J.M. Amado, J. Montero, and A. Yáñez, *Phys. Procedia* 83, 606 <https://doi.org/10.1016/j.phpro.2016.08.063> (2016).

8. V. Juechter, T. Scharowsky, R.F. Singer, and C. Körner, *Acta Mater.* 76(Supplement C), 252 <https://doi.org/10.1016/j.actamat.2014.05.037> (2014).
9. R.J. Hebert, *J. Mater. Sci.* 51(3), 1165 <https://doi.org/10.1007/s10853-015-9479-x> (2016).
10. H. Yu, S. Hayashi, K. Kakehi, and Y. L. Kuo, *Metals* <https://doi.org/10.3390/met9010019> (2019).
11. H.P. Tang, M. Qian, N. Liu, X.Z. Zhang, G.Y. Yang, and J. Wang, *JOM* 67(2), 555 <https://doi.org/10.1007/s11837-015-1300-4> (2015).
12. W.L. Finlay, and J.A. Snyder, *J. Metals* 188, 227 (1950).
13. L.C. Ardila, F. Garcíandia, J.B. Gonzalez Diaz, P. Alvarez, A. Echeverria, M.M. Petite, R. Deffley, J. Ochoa, L.C. Ardila, and F. Garcíandia, *Phys. Procedia* 56, 99 (2014).
14. L. Cordova, M. Campos, and T. Tinga, *JOM* 71, 1062 <https://doi.org/10.1007/s11837-018-3305-2> (2019).
15. Y. Sun, M. Aindow, and R.J. Hebert, *Mater. High Temp.* 35(1 3), 217 <https://doi.org/10.1080/09603409.2017.1389133> (2018).
16. J. Smialek, *Curr. Comput. Aided Drug Des.* <https://doi.org/10.3390/cryst11010060> (2021).
17. B.A. Pint, and J.H. Schneibel, *Scripta Mater.* 52(12), 1199 (2005).
18. A.W. Funkenbusch, J.G. Smeggil, and N.S. Bornstein, *Mettallurgical Trans. A* 16A, 1164 (1985).
19. W.R. Sun, S.R. Guo, J.H. Lee, N.K. Park, Y.S. Yoo, S.J. Choe, and Z.Q. Hu, *Mater. Sci. Eng., A* 247(1), 173 [https://doi.org/10.1016/S0921-5093\(97\)00753-3](https://doi.org/10.1016/S0921-5093(97)00753-3) (1998).
20. K.A. Unocic, L.M. Kolbus, R.R. Dehoff, S.N. Dryepondt, B.A. Pint *Corrosion* 2014 (4478).
21. M. Romedenne, R. Pillai, M. Kirka, and S. Dryepondt, *Corros. Sci.* 171, 108647 <https://doi.org/10.1016/j.corsci.2020.108647> (2020).
22. T. Sanviemvongsak, D. Monceau, M. Madelain, C. Desgranges, J. Smialek, and B. Macquaire, *Corros. Sci.* 192, 109804 <https://doi.org/10.1016/j.corsci.2021.109804> (2021).
23. N. Ramenatte, A. Vernouillet, S. Mathieu, A. Vande Put, M. Vilasi, and D. Monceau, *Corros. Sci.* 164, 108347 <https://doi.org/10.1016/j.corsci.2019.108347> (2020).
24. J. Sames, F. Medina, W.H. Peter, S.S. Babu, R.R. Dehoff, Effect of process control and powder quality on inconel 718 produced using electron beam melting, *8th International Symposium on Superalloy 718 and Derivatives*, John Wiley & Sons, Inc. 2014, pp. 409 423.
25. P. Tao, H. Li, B. Huang, Q. Hu, S. Gong, and Q. Xu, *Vacuum* 159, 382 <https://doi.org/10.1016/j.vacuum.2018.10.074> (2019).
26. A. Casadebaigt, J. Hugues, and D. Monceau, *Corros. Sci.* 175, 108875 (2020).
27. V.B. Trindade, U. Krupp, P.E.G. Wagenhuber, and H.J. Christ, *Mater. Corros. Werkstoffe Und Korrosion* 56(11), 785 (2005).
28. L. Li, X. Gong, X. Ye, J. Teng, Y. Nie, Y. Li, and Q. Lei, *Mater. (Basel)* 11(12), 2549 <https://doi.org/10.3390/ma11122549> (2018).
29. C. Juillet, A. Oudriss, J. Balmain, X. Feaugas, and F. Pedraza, *Corros. Sci.* 142, 266 <https://doi.org/10.1016/j.corsci.2018.07.032> (2018).
30. C. Siri, I. Popa, A. Vion, C. Langlade, and S. Chevalier, *Oxid. Met.* 94(5), 527 <https://doi.org/10.1007/s11085-020-1005-8> (2020).
31. Y. J. Kang, S. Yang, Y. K. Kim, B. AlMangour, and K. A. Lee, *Corros. Sci.* 158, 108082 <https://doi.org/10.1016/j.corsci.2019.06.030> (2019).
32. A. Strondl, O. Lyckfeldt, H. Brodin, and U. Ackelid, *JOM* 67(3), 549 <https://doi.org/10.1007/s11837-015-1304-0> (2015).
33. M.C. Kuner, M. Romedenne, P. Fernandez Zelaia, and S. Dryepondt, *Addit. Manuf.* 36, 101431 <https://doi.org/10.1016/j.addma.2020.101431> (2020).
34. A. Vernouillet, A. Vande Put, A. Pugliara, S. Doublet, and D. Monceau, *Corros. Sci.* 174, 108820 <https://doi.org/10.1016/j.corsci.2020.108820> (2020).
35. M.Y. He, A.G. Evans, and J.W. Hutchinson, *Mater. Sci. Eng., A* 245, 168 (1998).
36. G. Bertali, F. Scenini, and M.G. Burke, *Corros. Sci.* 111, 494 <https://doi.org/10.1016/j.corsci.2016.05.022> (2016).
37. A. Chyrkin, P. Huczowski, V. Shemet, L. Singheiser, W.J. Quadackers, (2011). Predicting subsurface enrichment depletion processes during high temperature oxidation of alloy 625 thin foils, *18th International Corrosion Congress*, Perth, Australia p. p. 456.
38. C. Romain, D. Texier, C. Desgranges, J. Cormier, S. Knittel, D. Monceau, and D. Delagnes, *Oxid. Met.* 96(1), 169 <https://doi.org/10.1007/s11085-021-10075-2> (2021).
39. D. Texier, Q. Sirvin, V. Velay, M. Salem, D. Monceau, B. Mazères, A. Andrieu, R. Roumiguier, B. Dod, *14th World Conference on Titanium, Nantes Juin 10 14, 2019, MATEC Web of Conferences*, 321, 06004 (2020). <https://doi.org/10.1051/mateconf/202032106004>.
40. A.B. Spierings, K. Dawson, T. Heeling, P.J. Uggowitzer, R. Schaublin, F. Palm, and K. Wegener, *Mater. Des.* 115, 52 <https://doi.org/10.1016/j.matdes.2016.11.040> (2017).
41. C. Hong, D. Gu, D. Dai, S. Cao, M. Alkhayat, Q. Jia, A. Gasser, A. Weisheit, I. Kelbassa, M. Zhong, and R. Poprawe, *J. Laser Appl.* 27(S1), S17005 <https://doi.org/10.2351/1.4898647> (2014).

**Publisher's Note** Springer Nature remains neutral with regard to jurisdictional claims in published maps and institutional affiliations.